Transverse-momentum fluctuations in relativistic heavy-ion collisions from event-by-event viscous hydrodynamics

Piotr Bożek[1, 2, *] and Wojciech Broniowski[1, 3, †]

[1] *The H. Niewodniczański Institute of Nuclear Physics, Polish Academy of Sciences, PL-31342 Kraków, Poland*
[2] *Institute of Physics, Rzeszów University, PL-35959 Rzeszów, Poland*
[3] *Institute of Physics, Jan Kochanowski University, PL-25406 Kielce, Poland*

(Dated: 8 March 2012)

We analyze event-by-event fluctuations of the transverse momentum in relativistic heavy-ion collisions at $\sqrt{s_{NN}} = 200$ GeV in the framework based on the fluctuating Glauber-model initial conditions, event-by-event $(3+1)$-dimensional viscous hydrodynamics, and statistical hadronization. We use the scaled fluctuation measure $\langle \Delta p_{Ti} \Delta p_{Tj} \rangle / \langle\langle p_T \rangle\rangle$. The identified "geometric" mechanism of generating the transverse-momentum fluctuations from the initial size fluctuations, transmitted to the final statistical-hadronization phase with hydrodynamics, is capable of easily reproducing the magnitude of the effect and explains the basic features of the data. On the other hand, it is somewhat too strong, hinting on modification of the popular Glauber approach to the earliest phase of the collision. We have checked that the considered measure is insensitive of the values of the shear and bulk viscosity coefficients, the freeze-out temperature, and the smoothing parameter for the initial distribution. It remains unaltered in the core-corona picture and is insensitive to the transverse-momentum conservation, approximately imposed in the statistical hadronization.

PACS numbers: 25.75.-q, 25.75.Gz, 25.75.Ld
Keywords: relativistic heavy-ion collisions, transverse-momentum fluctuations, Glauber models, wounded nucleons, viscous hydrodynamics, statistical hadronization, SPS, RHIC, LHC

I. INTRODUCTION

In Ref. [1] a new mechanism for generating the transverse-momentum fluctuations in relativistic heavy-ion collisions was identified. It is based on the random event-by-event fluctuations of the initial size of the formed system, its subsequent hydrodynamic evolution, and statistical hadronization. In the present work we further explore and extend this analysis, applying $(3+1)$-dimensional [$(3+1)$-D)] viscous event-by-event hydrodynamics. The basic idea of Ref. [1] is as follows: Even when we consider a very narrow centrality class of events, *e.g.*, with a strictly fixed number of wounded nucleons, N_w, the size of the initial fireball fluctuates event-by-event due to the random nature of the nuclear collision in the Glauber treatment. These fluctuations are then transferred by hydrodynamics to the fluctuations of the generated transverse flow velocity. At freeze-out, this translates into the event-by-event fluctuations of the average transverse momentum of hadrons produced in the event, $\langle p_T \rangle$. In essence, via simple scaling arguments, a more *squeezed* initial condition leads to more rapid expansion, larger velocity flow, and higher $\langle p_T \rangle$, while a *swollen* initial condition leads to slower expansion, lower flow, and lower $\langle p_T \rangle$. We will now explore this mechanism through the use of state-of-the-art tools, such as `GLISSANDO` [2] Monte Carlo code for the Glauber phase, $(3+1)$-D event-by-event viscous hydrodynamics [3, 4] for the dynamical evolution, and `THERMINATOR` [5, 6] for the statistical hadronization at freeze-out.

The event-by-event $\langle p_T \rangle$ fluctuations in relativistic collisions have been actively studied theoretically [7–26] and experimentally [27–38], as they may reveal relevant details of the dynamics of the system, more accurate than contained in the one-body observables. Moreover, they are expected be sensitive to the critical phenomena at the phase transition, providing an important probe for these effects.

Throughout the paper we use the notation

$$\langle . \rangle, \quad \langle\langle . \rangle\rangle \tag{1}$$

to indicate averaging in a given event, and averaging of the single-event averages over all events, respectively.

The structure of the paper is as follows: in Sec. II we give the details of the Monte Carlo simulations of the initial phase, focusing on the size fluctuations, Sec. III provides some necessary description of the applied $(3+1)$-D viscous hydrodynamics, while the statistical hadronization is described in Sec. IV. We then proceed in Sec. V to presenting the results, which are compared to the data from the STAR and PHENIX collaborations. We investigate the influence of model details on the results of our calculation, finding them very robust. In particular, the STAR measure of the event-by-event transverse momentum fluctuations is insensitive to the medium viscosity, freeze-out temperature, or the smoothing parameter of the initial distribution of sources. Our final conclusions and discussion is contained in Sec. VI.

* Piotr.Bozek@ifj.edu.pl
† Wojciech.Broniowski@ifj.edu.pl

II. INITIAL STATE FLUCTUATIONS IN THE GLAUBER APPROACH

The initial condition for hydrodynamics may be obtained from the Glauber approach, leading to the successful wounded-nucleon picture [39, 40] (a wounded nucleon is a nucleon that collided inelastically at least once) or its descendants, such as the *mixed* model [2, 41]. When the initial condition is obtained via Glauber Monte Carlo simulations, the distribution of sources (wounded nucleons or positions of binary collisions) in the transverse plane *fluctuates*, reflecting the randomness in positions of the nucleons in the colliding nuclei. This leads to fluctuations of *shape*.

The event-by-event fluctuations of the elliptic component of initial shape have been actively studied, as they lead to significantly enhanced elliptic flow [26, 42–53]. They also generate odd Fourier components, absent from the event-averaged studies, such as the triangular deformation [54–56], as well as higher-order components of the flow. Other interesting phenomena appear as the result of fluctuations, *e.g.*, the torque effect [57] of the reaction planes at forward and backward pseudorapidities, or the directed flow at central rapidity [58, 59].

We now describe in some detail the implementation of the Glauber model used in this work. The density of charged particles per unit of pseudorapidity, as a function of centrality, can be parametrized using a formula [41, 60, 61] incorporating an admixture of binary collisions, $N_{\rm bin}$, into the wounded-nucleon model in the following way:

$$\frac{dN_{\rm charged}}{d\eta} \propto \left(\frac{1-\alpha}{2}N_w + \alpha N_{\rm bin}\right), \qquad (2)$$

where α is a phenomenological parameter, $\alpha = 0.145$ for the highest RHIC energy of $\sqrt{s_{NN}} = 200$ GeV [61]. The initial-state simulations are carried out with `GLISSANDO` [2], including a component from binary collisions. The parameter α in the initial distribution is somewhat smaller from the value extracted from the final distributions (see the following). The difference is due to the longitudinal expansion and entropy production in the $(3+1)$-D viscous hydrodynamic expansion [3].

The positions of nucleons in each of the colliding nuclei are randomly generated from a Woods-Saxon distribution, with an additional constraint enforcing the short-range repulsion, namely, that the centers of nucleons in each nucleus cannot be generated closer than the expulsion distance $d = 0.9$ fm. Nucleons from the two colliding nuclei are wounded, or a binary collision occurs, when their centers get closer to each other than the distance $\sqrt{\sigma^{\rm inel}_{NN}/\pi}$, with $\sigma^{\rm inel}_{NN}$ denoting the inelastic nucleon-nucleon cross section. For the highest RHIC energy of $\sqrt{s_{NN}} = 200$ GeV one has $\sigma^{\rm inel}_{NN} = 42$ mb.[1]

[1] One may more appropriately use a Gaussian wounding profile instead of the applied hard-sphere wounding profile, but the results do not differ significantly in the case of size fluctuations [62].

The notion of sources, originally limited to the transverse plane, may be extended on the rapidity dependence of the particle emission. Although this extension is not crucial for the present study, focused on the mid-rapidity region, we include it for the integrity of the paper. The spatial pseudorapidity ($\eta_\parallel$) distribution of the emission profile is given as the sum of contributions from the forward- and backward-moving wounded nucleons. Within such an extended framework Białas and Czyż have properly described [63] the pseudorapidity distributions of charged particles in the $d-Au$ collisions. Therefore, we assume an asymmetric emission profile [63, 64] peaked in the forward (backward) rapidity for the forward (backward) moving wounded nucleons, denoted as $f_+(\eta_\parallel)$ ($f_-(\eta_\parallel)$),

$$f_\pm(\eta_\parallel) = \left(1 \pm \frac{\eta_\parallel}{y_{\rm beam}}\right) f(\eta_\parallel), \qquad (3)$$

where $y_{\rm beam}$ is the beam rapidity. The initial profile in space-time rapidity is

$$f(\eta_\parallel) = \exp\left(-\frac{(\eta_\parallel - \eta_0)^2}{2\sigma_\eta^2}\theta(|\eta_\parallel| - \eta_0)\right), \qquad (4)$$

with $\eta_0 = 1.5$, $\sigma_\eta = 1.4$ [3]. The initial entropy density is assumed to have a factorized form

$$s(x, y, \eta_\parallel) = \kappa \sum_i f_\pm(\eta_\parallel) g_i(x, y) \left[(1-\alpha) + N_i^{coll}\alpha\right]. \qquad (5)$$

Here N_i^{coll} is the number of collisions of the participant nucleon i, and

$$g_i(x, y) = \frac{1}{2\pi w^2} \exp\left[-\frac{(x-x_i)^2 + (y-y_i)^2}{2w^2}\right]. \qquad (6)$$

implements a Gaussian smearing, replacing the point-like source at the transverse position (x_i, y_i) with a Gaussian profile. The smearing parameter is taken to be $w = 0.4$ fm, and the overall scale factor is $\kappa = 2.5$ GeV. The parameter α of the mixed model is fixed to reproduce the dependence of $dN/d\eta$ on centrality. In the $(3+1)$-D viscous hydrodynamic model the optimum value is $\alpha = 0.125$ at the top RHIC energies [3]. We remark that the mixed model works also very well for the description of multiplicities a the LHC energy of $\sqrt{s_{NN}} = 2.76$ TeV, where $\alpha = 0.15$ [65, 66].

In Fig. 1 we show two snapshots of typical configurations of sources in the transverse plane generated with `GLISSANDO`. The dots indicate the positions of the wounded nucleons. Since we have in mind the distributions as starting conditions for the event-by-event hydrodynamics, we need to smear out the point-like distributions. The smearing procedure, although physically motivated and necessary, is somewhat arbitrary in introducing a smearing scale. In Fig. 1, the contours show the smeared entropy density, s, with $w = 0.4$ fm. Although both selected events correspond to the same number of

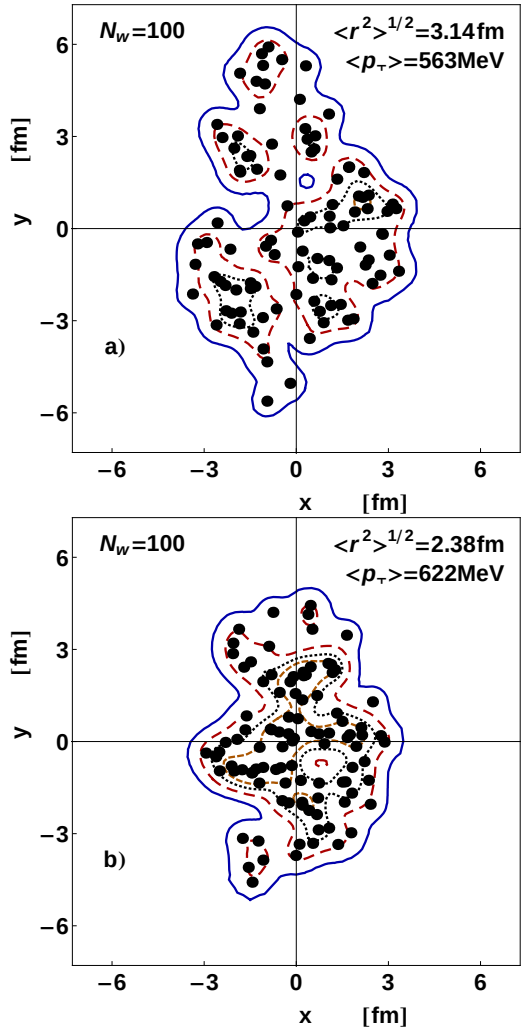

FIG. 1. (Color online) Two typical configuration of wounded nucleons in the transverse plane (dots) generated with GLISSANDO and the corresponding contours of the smeared density of entropy, s. Solid, dashed, and dotted lines correspond to isentropes at $s = 0.05$, 0.2, and 0.4 GeV^{-3}, respectively. The densities for the two events have radically different r.m.s. radii of 3.14 and 2.38 fm, respectively, despite the equal number of the wounded nucleons, $N_w = 100$.

wounded nucleons, $N_w = 100$, they have radically different r.m.s. radii, which after the hydrodynamic expansion results in different transverse flows.

To have a simple size measure we look at the average transverse size of the initial fireball, defined in each event via the mean squared radius at the central space-time rapidity

$$\langle r^2\rangle \equiv \frac{\int dxdy(x^2+y^2)s(x,y,0)}{\int dxdy\ s(x,y,0)}\ . \tag{7}$$

In the following we use the notation $\langle r\rangle \equiv \langle r^2\rangle^{1/2}$. The point, clearly seen from Fig. 1, is that even at precisely fixed centrality the size $\langle r\rangle$ fluctuates [1]. The feature is presented quantitatively in Fig. 2, where we plot the event-by event scaled standard deviation of $\langle r\rangle$ obtained

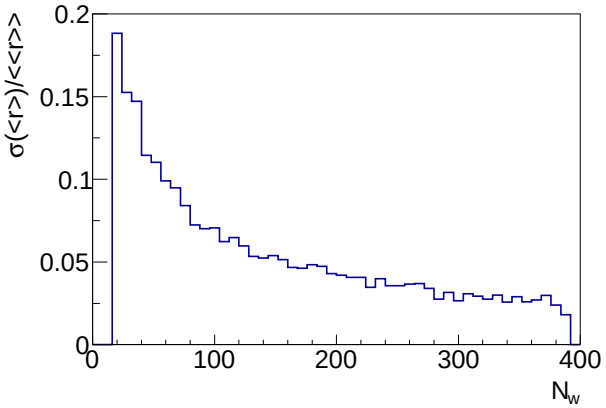

FIG. 2. (Color online) Event-by-event scaled standard deviation of the size parameter $\langle r\rangle$, evaluated at fixed values of the number of wounded nucleons N_w from the initial entropy density for events used in hydrodynamic simulations.

at each N_w. As expected, $\sigma(\langle r\rangle)/\langle\langle r\rangle\rangle$ is a decreasing function of N_w.

As noted in Ref. [1], very similar curves to Fig. 2 are obtained for other variants of Glauber models, such as models with overlaid distributions of particles produced from the sources [2], simulations applying a Gaussian wounding profile [67] for the NN collisions, or the use of the nucleon distributions including realistic (central) NN correlations of Ref. [68–70]. This means that the behavior of the initial geometry shown in Fig. 2 is robust, essentially reflecting the statistical feature of the Glauber approach.

III. VISCOUS EVENT-BY-EVENT HYDRODYNAMICS

It is widely believed that a successful and uniform description of the physics of relativistic heavy-ion collisions is achieved with the help of relativistic hydrodynamics (for reviews see, e.g., [71–73]). *Event-by-event* hydrodynamic calculations for fluctuating initial conditions have been performed for perfect fluid [47, 56, 59, 74–76] and for the viscous case [4, 77–79], focusing on collective flow.

In the second-order *viscous* hydrodynamic formalism [80–82], the hydrodynamic equations

$$\partial_\mu T^{\mu\nu} = 0 \tag{8}$$

with the energy-momentum tensor

$$T^{\mu\nu} = (\epsilon + p)u^\mu u^\nu - pg^{\mu\nu} + \pi^{\mu\nu} + \Pi\Delta^{\mu\nu} \tag{9}$$

are supplemented with equations for the stress corrections from the shear,

$$\Delta^{\mu\alpha}\Delta^{\nu\beta}u^\gamma\partial_\gamma\pi_{\alpha\beta} = \frac{2\eta\sigma^{\mu\nu}-\pi^{\mu\nu}}{\tau_\pi} - \frac{4}{3}\pi^{\mu\nu}\partial_\alpha u^\alpha, \tag{10}$$

and the bulk viscosity,

$$u^\gamma \partial_\gamma \Pi = \frac{-\zeta \partial_\gamma u^\gamma - \Pi}{\tau_\Pi} - \frac{4}{3}\Pi \partial_\alpha u^\alpha, \tag{11}$$
$$\sigma_{\mu\nu} = \frac{1}{2}\left(\nabla_\mu u_\nu + \nabla_\mu u_\nu - \frac{2}{3}\Delta_{\mu\nu}\partial_\alpha u^\alpha\right).$$

Here $\nabla^\mu = \Delta^{\mu\nu}\partial_\nu$, while η and ζ denote the shear and bulk viscosity coefficients, respectively. In our default calculations we use constant $\eta/s = 0.08$, $\zeta/s = 0.04$ in the hadronic phase, $\tau_\pi = 3\eta/(Ts)$, and $\tau_\Pi = \tau_\pi$. To test the sensitivity of our results on viscosity, we perform calculations for $\eta/s = 0.16$, $\zeta/s = 0.04$ and $\eta/s = 0.08$, $\zeta/s = 0.08$ as well.

The applied equation of state is a *crossover* equation of state, interpolating between the lattice-QCD results at high temperatures [83] and a hadronic gas equation of state at low temperatures. The construction of the equation of state follows the method of Chojnacki and Florkowski [84] (for details see [3]).

In this work we apply the event-by-event (3 + 1)-D viscous hydrodynamics [4, 77], starting the evolution at 0.6 fm/c. The configurations of wounded nucleons and binary collisions corresponding to the centrality range $0 - 70\%$ are generated with `GLISSANDO`. The procedure does not fix the impact parameter for each centrality bin, as the Monte-Carlo scheme picks the impact parameter in each event according to the distribution $P(b) = d\sigma_{inel}(b)/(db\,\sigma_{inel})$ [2][85]. For each configuration of wounded nucleons a hydrodynamic evolution is calculated starting from the density (5).

IV. STATISTICAL HADRONIZATION

The last stage of our approach is the simulation of the statistical hadronization at freeze-out [86] (for a review, see, e.g. [73]) with `THERMINATOR` [5, 6]. The code includes all resonances and decay channels from `SHARE` [87]. The particles (stable and unstable, which subsequently decay) are formed at the freeze-out hypersurface according to the Frye-Cooper formula. In the case of viscous hydrodynamics, the momentum distributions at freeze-out are modified by the viscous corrections. The shear and bulk viscosity corrections are [88]

$$\delta f_{shear} = f_0\,(1 \pm f_0)\,\frac{1}{2T^2(\epsilon + p)} p^\mu p^\nu \pi_{\mu\nu} \tag{12}$$

and [89, 90],

$$\delta f_{bulk} = C_{bulk} f_0\,(1 \pm f_0)\left(c_s^2 u^\mu p_\mu - \frac{(u^\mu p_\mu)^2 - m^2}{3u^\mu p_\mu}\right)\Pi, \tag{13}$$

[2] This is simply achieved by generating a uniform distribution in b^2 and accepting those events where at least one NN interaction occurred.

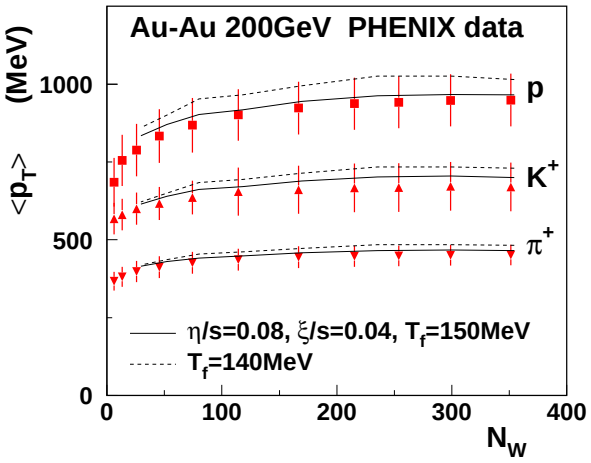

FIG. 3. (Color online) Averaged inclusive transverse momentum vs. number of wounded nucleons, N_w. The data (extrapolated to the whole p_T range) come from the PHENIX Collaboration [92] and show the charged pions (down triangle), charged kaons (up triangles), and protons and antiprotons (squares). The lines correspond to our model calculation with $\eta/s = 0.08$, $\zeta/s = 0.04$, and $T_f = 150$ MeV (solid lines), and $T_f = 140$ MeV (dashed lines).

respectively, with f_0 denoting the equilibrium distributions and c_s standing for the velocity of sound. In the local rest frame the normalization constant is

$$\frac{1}{C_{bulk}} = \frac{1}{3}\sum_n \int \frac{d^3p}{(2\pi)^3}\frac{m^2}{E} f_0\,(1 \pm f_0)\left(c_s^2 E - \frac{p^2}{3E}\right), \tag{14}$$

where the sum runs over all the hadron species. The (single-fluid) hydrodynamic evolution uses an equation of state with zero chemical potentials. However, the chemical potentials are reintroduced in the Frye-Cooper formula with the ratio μ/T fixed through the fits to the particle ratios at the chemical freeze-out, which works properly at the RHIC energies [91].

Before showing the p_T-correlation results, let us state that our approach properly describes the relevant one-body features of the collisions, in particular, the transverse-momentum spectra. As an example, in Fig. 3 we show the inclusive average transverse momentum as the function of N_w for pions, kaons, and protons and antiprotons for our default parameters $T_f = 150$ MeV, $\eta/s = 0.08$, $\zeta/s = 0.04$ (solid lines). The result compares favorably to the PHENIX data [92]. The agreement is important, as it shows that we have the correct one-body background to study correlations. Fixing the freeze-out temperature of $T_f = 150$ MeV reproduces the transverse momenta of identified particles at midrapidity. To check the sensitivity of the results of the freeze-out temperature and viscosity, we have investigated also the cases when one of the parameter is modified from the default

value to $T_f = 140$ MeV, $\eta/s = 0.16$, or $\zeta/s = 0.08$. The calculations with a lower freeze-out temperature or with an increased shear or bulk viscosity give average transverse momenta within the range of the systematic errors quoted by the PHENIX Collaboration. Admittedly, there is some model dependence on parameters, but it is weak, and the default parameters serve as an optimum choice.

It has been noted that event-by-event hydrodynamics with lumpy initial conditions yields harder spectra than hydrodynamics starting with averaged initial conditions [93]. This effect follows from higher gradients in the lumpy initial condition. To compensate, i.e., to soften the spectra, one needs to run hydrodynamics for a shorter time, i.e., to higher freeze-out temperatures [3].

V. RESULTS

The simulations presented in this section employ the experimental cuts in the STAR [32] (0.15 GeV $< p_T <$ 2 GeV) and PHENIX [29] (0.2 GeV $< p_T <$ 2 GeV) analyses. In both cases $|\eta| < 1$. Our samples have 100 events at each considered centrality bin. These, involving the hydrodynamic evolution, are time-consuming to generate. To increase the accuracy of the statistical hadronization, we generate 200 `THERMINATOR` events for each hydro event.

Our determination of centrality matches closely the experiment. In the case of STAR [32], the multiplicity of generated charged particles in the window $|\eta| < 0.5$ is used to determine the centrality bins. In the case of PHENIX [29], where a combination of signals from the BBC and ZDC detectors is used, we simply take the number of wounded nucleons N_w as the variable fixing the centrality.

A. Fixed number of wounded nucleons

For better understanding, we begin the analysis for the event-by-event fluctuations by selecting a very narrow centrality class, with $N_w = 100$. We run `GLISSANDO` to generate the initial conditions, carry out our event-by-event hydrodynamics, and, finally, run `THERMINATOR` and compute $\langle p_T \rangle$ in each event. As argued before [1], the fluctuations of the initial condition manifest themselves in the fluctuations of the initial size $\langle r \rangle$. In Fig. 4 we plot the values of $\langle p_T \rangle$, histogrammed in bins of $\langle r \rangle$. Each point corresponds to one event, while the bars give the event-by-event average, $\langle\langle p_T \rangle\rangle$. We note a clear anticorrelation of $\langle\langle p_T \rangle\rangle$ and $\langle\langle r \rangle\rangle$. This shows that in a full-fledged event-by-event simulation the basis qualitative argument holds: for a squeezed initial the system expands with the larger flow velocity hand acquires a higher average transverse momentum, $\langle\langle p_T \rangle\rangle$, than for the stretched state. The same effect can be observed when comparing case by case events generated from different initial conditions (Fig. 1). The event with a squeezed initial density has a larger transverse flow and $\langle p_T \rangle$.

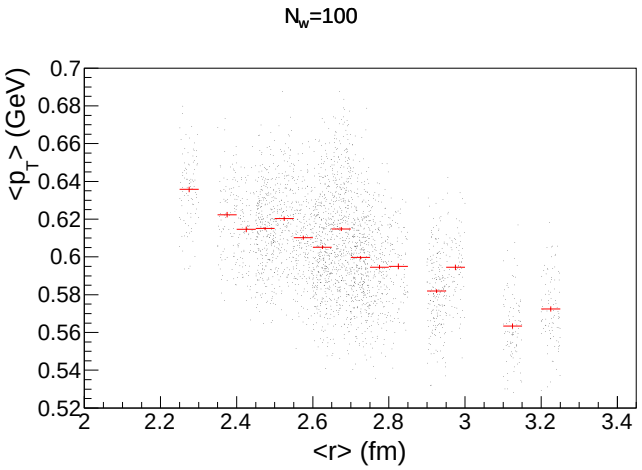

FIG. 4. (Color online) Averaged transverse momentum as the function of the initial size $\langle r \rangle$ for events with a fixed number of wounded nucleons, $N_w = 100$. Viscous $(3+1)$-D event-by-event hydrodynamics with $\eta/s = 0.08$, $\zeta/s = 0.04$, and $T_f = 150$ MeV is used. The scattered small dots show $\langle p_T \rangle$ obtained in individual events, while the bars show the event-by-event averages $\langle\langle p_T \rangle\rangle$ in the selected bins of $\langle r \rangle$. The anticorrelation is apparent, with lower size $\langle r \rangle$ resulting in higher $\langle\langle p_T \rangle\rangle$.

The fit to the histogram bars in Fig. 4 yields $\langle\langle p_T \rangle\rangle = 0.79 - 0.07\langle\langle r \rangle\rangle$ GeV/fm, which in turn gives

$$\frac{d\langle\langle p_T \rangle\rangle}{d\langle\langle r \rangle\rangle} \simeq -0.3 \frac{\langle\langle p_T \rangle\rangle}{\langle\langle r \rangle\rangle} \tag{15}$$

in the considered range. This result can be written as

$$\frac{\sigma(\langle p_T \rangle)}{\langle\langle p_T \rangle\rangle} \simeq 0.3 \frac{\sigma(\langle r \rangle)}{\langle\langle r \rangle\rangle}, \tag{16}$$

which may be compared to the estimate of Ref. [94],

$$\frac{\sigma(\langle p_T \rangle)}{\langle\langle p_T \rangle\rangle} = \frac{2\bar{P}}{\bar{\epsilon}} \frac{\sigma(\langle r \rangle)}{\langle\langle r \rangle\rangle}, \tag{17}$$

with $\bar{P}$ and $\bar{\epsilon}$ denoting the average pressure and energy density during the evolution of the system. Thus $\bar{P}/\bar{\epsilon} \sim 0.15$, which is the right ball park for the applied equation of state [95].

B. Transverse momentum fluctuations vs. centrality

Now we come to the main results of this paper. In order to compare to the data, we analyze the STAR correlation measure [32], $\langle \Delta p_{Ti} \Delta p_{Tj} \rangle$, defined as

$$\langle \Delta p_{Ti} \Delta p_{Tj} \rangle \equiv \frac{1}{N_{\rm ev}} \sum_{k=1}^{N_{\rm ev}} \frac{C_k}{N_k(N_k-1)}, \tag{18}$$

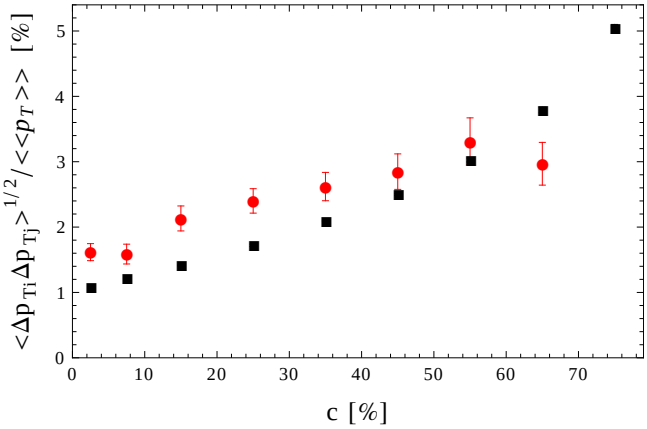

FIG. 5. (Color online) Comparison of the theoretical predictions for $\langle \Delta p_{Ti} \Delta p_{Tj} \rangle^{1/2} / \langle\langle p_T \rangle\rangle$ (for $\sqrt{s_{NN}} = 200$ GeV) to the experimental data extracted from the STAR Collaboration [32] (squares). The dots correspond to simulation with event-by-event (3+1)−D viscous hydrodynamics with our default parameters $T_f = 150$ MeV, $\eta/s = 0.08$, $\zeta/s = 0.04$. The statistical errors of the model simulation are obtained with the jackknife method. The experimental statistical errors are negligible.

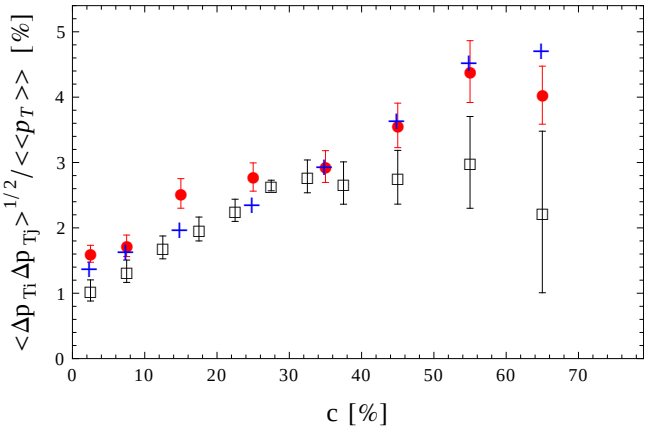

FIG. 6. (Color online) Comparison of the theoretical predictions for $\langle \Delta p_{Ti} \Delta p_{Tj} \rangle^{1/2} / \langle\langle p_T \rangle\rangle$ (for $\sqrt{s_{NN}} = 200$ GeV) to the experimental data from the PHENIX Collaboration [29] (squares). The dots correspond to simulation with event-by-event $(3+1)$-D viscous hydrodynamics with our default parameters $T_f = 150$ MeV, $\eta/s = 0.08$, $\zeta/s = 0.04$. The crosses indicate the approximate result from Ref. [1] for perfect (2+1)-D hydrodynamics with averaged initial conditions from the mixed model. The statistical errors for the model simulations are obtained with the jackknife method.

where $N_{\rm ev}$ is the number of events, N_k the multiplicity in event k, and

$$C_k = \sum_{i=1}^{N_k} \sum_{j=1, j\neq i}^{N_k} (p_i - \langle\langle p_T \rangle\rangle)(p_j - \langle\langle p_T \rangle\rangle), \qquad (19)$$

with

$$\langle\langle p_T \rangle\rangle = \frac{1}{N_{\rm ev}} \sum_{k=1}^{N_{\rm ev}} \langle p_T \rangle_k. \qquad (20)$$

Introducing the mean momentum in event k, denoted by $\langle p_T \rangle_k$, we can transform

$$C_k = N_k(N_k - 1)(\langle p_T \rangle_k - \langle\langle p_T \rangle\rangle)^2 - \sum_{i=1}^{N_k} (p_i - \langle p_T \rangle_k)^2, \qquad (21)$$

and rewrite

$$\langle \Delta p_{Ti} \Delta p_{Tj} \rangle = \frac{N_{\rm ev} - 1}{N_{\rm ev}} {\rm var}(\langle p_T \rangle) - \frac{1}{N_{\rm ev}} \sum_{k=1}^{N_{\rm ev}} \left[\frac{{\rm var}_k(p)}{N_k} \right]. \qquad (22)$$

Thus the STAR correlation measure is the difference of two terms: one involving the variance of the mean momenta in events, and the other being the event-averaged variance of the momentum in each event decided by the multiplicity of this event. Note that expression (22) involves only single sums in a given event. As a matter of fact, the STAR analysis [32] replaces $\langle\langle p_T \rangle\rangle$ with the quantity $\langle p_T \rangle(N_{\rm charged})$, the average momentum as a function of the number of charged particles in the pseudorapidity bin $|\eta| < 0.5$ – the same as used to determine centrality. The function is obtained by a numerical fit to the results prior to the analysis of the correlations. The method slightly reduces the value of $\langle \Delta p_{Ti} \Delta p_{Tj} \rangle$. We follow the same prescription.

Our results are shown in Fig. 5, where we compare the theoretical points (circles) to the experimental data from the STAR Collaboration [32] (squares). At low centralities, the model calculations overshoot the data by about 50%, yielding more p_T fluctuations than needed. This conclusion supports the original findings of Ref. [1] in the present state-of-the-art event-by-event treatment. We have checked for a few centrality bins that modifying the shear or bulk viscosity coefficients, the freeze-out temperature or the width of the smearing Gaussian in the initial conditions does not change the results at the level of the statistical errors of our calculations (see sect. V C).

Nevertheless, we note a proper magnitude of the effect and the correct dependence on centrality, Also, since the results of Fig. 2 very weakly depend on σ_{NN} [1], with the expectation that the hydrodynamic "push" is similar at different collision energies, our results should weakly depend on the incident energy. This is a desired feature, as the STAR data [32] are very similar from $\sqrt{s_{NN}} =$ 20 GeV to 200 GeV.

The statistical errors of the model simulations in Fig. 5 are estimated with the jackknife method. Essentially, the relative error is equal to $1/\sqrt{2n}$, where $n = 100$ is the number of the hydrodynamic events in the considered centrality class.

The PHENIX Collaboration [29] published results on the ratio of the p_T fluctuations using the measure

$$F_{p_T} = \frac{\omega_{p_T}^{\rm data} - \omega_{p_T}^{\rm mixed}}{\omega_{p_T}^{\rm mixed}}, \qquad (23)$$

where

$$\omega_{p_T}^{\rm data} = \frac{{\rm var}(\langle p_T \rangle)^{1/2}}{\langle\langle p_T \rangle\rangle} \tag{24}$$

and $\omega_{p_T}^{mixed}$ is the same quantity obtained with mixed events. For small dynamical fluctuations and sharp distributions in the multiplicity variable one can estimate[3]

$$\langle \Delta p_{Ti} \Delta p_{Tj} \rangle \simeq 2 F_{p_T} \frac{{\rm var}(p_T)}{\langle N \rangle}, \tag{25}$$

where var(p_T) denotes the inclusive variance of the transverse momentum distribution, and $\langle N \rangle$ is the average multiplicity of the detected particles in the considered centrality class. The values of the quantities on the right-hand side of Eq. (25) are available from the PHENIX Collaboration web page associated with Ref. [29]. We stress that the result Eq. (25) is approximate, but sufficiently accurate [96] for our purpose. A more direct comparison to the PHENIX data could be achieved with the mixing technique, however, this is beyond our reach due to a very limited number of the model events.

The result of the analysis is shown in Fig. 6, with similar conclusions as from Fig. 5, i.e., the model points are above the experiment. We also show that the results of applying the event-by-event viscous hydrodynamics (dots) are very close to the approximate calculation of Ref. [1] for perfect $(2+1)$-D hydrodynamics with averaged initial conditions (crosses).

The dependence of the fluctuation measure $\langle \Delta p_{Ti} \Delta p_{Tj} \rangle^{1/2} / \langle\langle p_T \rangle\rangle$ on the upper transverse-momentum cut-off has been measured by the PHENIX Collaboration [29]. As can be seen in Fig. 7, the fluctuations in the model increase with the cut-off, following closely the trend observed in the data. This cross-checks that the observed p_T-dependence of the transverse momentum fluctuations can be interpreted as a hydrodynamic flow effect.

C. Dependence on model parameters

In this section we investigate the dependence of our predictions on the model parameters, such as the viscosity coefficients of the medium, the freeze-out temperature, T_f, or the smoothing parameter, w. For this purpose we have run simulations with various values of these parameters at fixed $N_w = 100$.

In Fig. 8 we compare the dependence of $\langle p_T \rangle$ on $\langle r \rangle$ for several variants of viscous hydrodynamics. The points correspond to mean $\langle\langle p_T \rangle\rangle$ in a given $\langle r \rangle$ bin, and the

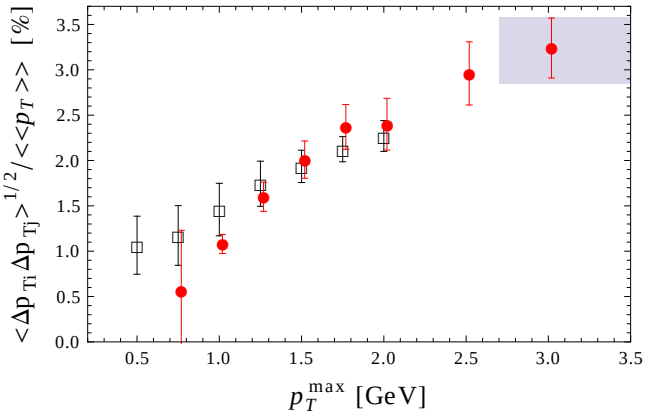

FIG. 7. (Color online) Dependence of $\langle \Delta p_{Ti} \Delta p_{Tj} \rangle^{1/2} / \langle\langle p_T \rangle\rangle$ (for $\sqrt{s_{NN}} = 200$ GeV) on the upper transverse-momentum cut-off, compared to the experimental data from the PHENIX Collaboration [29] for centrality $20-25\%$ (squares). The dots correspond to simulation with event-by-event (3+1)-D viscous hydrodynamics with our default parameters $T_f = 150$ MeV, $\eta/s = 0.08$, $\zeta/s = 0.04$. The statistical errors of the model simulation are obtained with the jackknife method. The shaded band in the upper right corner represents the error band of the result of the simulation with an infinite upper momentum cut-off.

curves are linear fits to these points. Our default result is for the set of parameters $\eta/s = 0.08$, $\zeta/s = 0.04$, $T_f = 150$ MeV, and $w = 0.4$ fm, indicated with the up-triangles and dot-dashed line in the plot. We then do our comparison by changing one of the parameters: the shear or bulk viscosity coefficient, the freeze-out temperature, or the smoothing parameter. As expected, increasing the shear viscosity or decreasing the freeze-out temperature leads to a hardening of the spectra, i.e, higher $\langle\langle p_T \rangle\rangle$. On the other hand, increasing bulk viscosity leads to a reduction of the effective pressure and a decrease of the average transverse momentum. Increasing the smearing width of the initial density distribution yields smaller gradients, and reduces the transverse push. The described behavior holds bin-by-bin in the $\langle r \rangle$ variable giving the size of the initial geometry.

At the same time we note that the slope of the dependence of $\langle\langle p_T \rangle\rangle$ on $\langle r \rangle$ changes as well. For all the studied cases it turns out that to a high accuracy

$$\frac{d\langle p_T \rangle}{d\langle r \rangle} \frac{\langle r \rangle}{\langle p_T \rangle} \simeq 0.31. \tag{26}$$

As a result, according to the arguments of Sec. V A, the scaled measure $\langle \Delta p_{Ti} \Delta p_{Tj} \rangle / \langle\langle p_T \rangle\rangle^2$ is hardly modified. Increasing the transverse pressure or the local gradients gives a larger transverse flow and, simultaneously, larger fluctuations, such that the scaled fluctuations of the transverse momentum practically do not depend on viscosity, the freeze-out temperature, or the smearing of the initial conditions. We thus find that the scaled p_T-fluctuations are dominated by the fluctuations of the transverse size of the initial fireball. This feature makes the scaled measure particularly suitable for constraining

[3] The relations between various popular correlations measures in this limit are discussed in the Appendix of Ref. [96]. One of us (WB) thanks Jeff T. Mitchell for the discussion concerning Eq. (23)

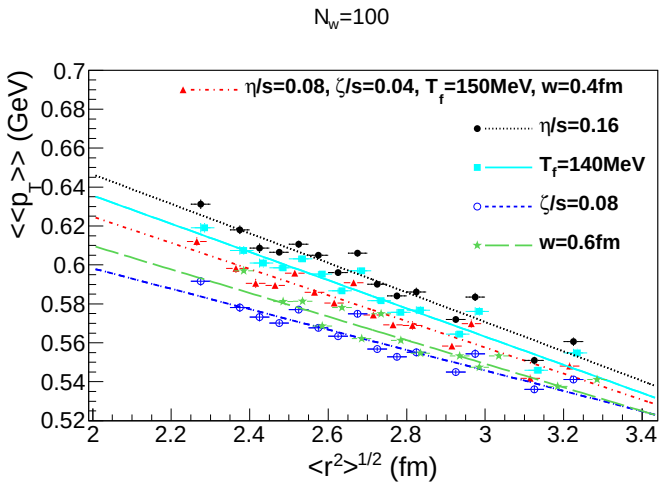

FIG. 8. (Color online) Dependence of $\langle\langle p_T\rangle\rangle$ on $\langle r\rangle$ for the variants of the hydrodynamic evolution: calculation with $\eta/s = 0.08$, $\zeta/s = 0.04$, $T_f = 150$ MeV, and $w = 0.4$ fm (default) (triangles and dashed-dotted line), with $\eta/s = 0.16$ (filled circles and dotted line), with $T_f = 140$ MeV (squares and solid line), with $\zeta/s = 0.08$ (open circles and dashed line), and with the width of the smearing $w = 0.6$ fm (stars and long dashed line). The points with the errors bars represent the histogram of the average momentum $\langle\langle p_T\rangle\rangle$ as function of the r.m.s radius of the initial density of the event. The lines represent linear fits to the points.

the models of the initial phase. In a similar way, the directed flow at central rapidity has been proposed as a tool to limit the dipole deformation of the fireball predicted by different models of the initial state [97].

D. Other effects

In peripheral collisions the particle emission can take place in the thermalized, collectively expanding core, as well as in the outer corona, where rescattering is small [98–101]. In the following we estimate the transverse momentum fluctuations in the case where the particles are emitted from these two sources, the core and the corona. Different definitions of the dense core are possible; we use the prescription that a wounded nucleon belongs to the core if it collides more than once. This choice of the separation between the core and the corona describes the centrality dependence of the strangeness production and of the effective slopes of the particle spectra [99, 102]. The particle density at central rapidity is a sum of the contributions from the corona and the core,

$$\frac{dN_{\rm charged}}{d\eta} = \frac{dN^{NN}_{\rm charged}}{d\eta}(N_{\rm corona} + \beta N_{\rm core}), \qquad (27)$$

with $N_{\rm core} + N_{\rm corona} = N_w$. To reproduce the centrality dependence observed experimentally we choose the parameter $\beta = 1.75$, which effectively describes the enhanced production in the thermalized matter [100]. The average transverse momentum,

$$\langle\langle p_T\rangle\rangle = (1-c)\langle\langle p_T^{pp}\rangle\rangle + c\langle\langle p_T^{\rm core}\rangle\rangle, \qquad (28)$$

is a combination of the average momentum in a NN-collision and of the average transverse momentum of particles emitted from the core. The fraction of particles emitted from the core is $c = \beta N_{\rm core}/(\beta N_{\rm core} + N_{\rm corona})$. By neglecting the fluctuations of the number of nucleons in the core, we get

$$\begin{aligned}\langle\Delta p_{Ti}\Delta p_{Tj}\rangle \simeq{}& \frac{1}{\langle N_{\rm corona}\rangle}(1-c)^2\langle\Delta p_{Ti}\Delta p_{Tj}\rangle^{NN} \\ &+ c^2(1-c)^2(\langle\langle p_T^{NN}\rangle\rangle - \langle\langle p_T^{\rm core}\rangle\rangle)^2 \\ &+ c^2\langle\Delta p_{Ti}\Delta p_{Tj}\rangle^{\rm core}. \qquad (29)\end{aligned}$$

The first term is a contribution from the $N_{\rm corona}$ independent NN sources, the second term comes from the difference of the transverse momenta from the two sources, and the third term is a contribution from the hydrodynamically expanding core. We use the PHENIX data [29] on the average transverse momentum and its fluctuations in the pp-collisions, and take for $\langle\Delta p_{Ti}\Delta p_{Tj}\rangle^{\rm core}$ the results from the hydrodynamic model calculation. With all elements of Eq. (29) combined, we find that $\langle\Delta p_{Ti}\Delta p_{Tj}\rangle^{1/2}/\langle\langle p_T\rangle\rangle$ is changed very little compared to the results of Sec. V B. For the most central collisions, where the corona contribution is tiny, naturally the effect is negligible. In peripheral collisions ($c = 60-70\%$) all terms of Eq. (29) contribute to the transverse momentum fluctuations. However, in the last term the reduction of the core due to the $(1-c)^2$ factor is compensated with increased fluctuations $\sigma(\langle r\rangle)/\langle r\rangle$, such that with all terms combined the change is at the level of 10%. At intermediate centralities the reduction effect is at a similar level. Therefore the core-corona model does not improve nor deteriorate the agreement with the experimental data.

We have also checked that imposing a finite detector acceptance, by simply accepting a simulated particle with the typical probability of 50%, does not alter the results for $\langle\Delta p_{Ti}\Delta p_{Tj}\rangle/\langle\langle p_T\rangle\rangle$. This is a feature of the scaled p_T fluctuation measure [29, 37].

Finally, we have estimated the possible effect of the global transverse-momentum conservation, not implemented in the standard simulations of the statistical hadronization with `THERMINATOR`. This can be approximately achieved by accepting only those events which have limited total transverse momentum. Specifically, we consider the quantity $P^2 = (\sum p_{i,x})^2 + (\sum p_{i,y})^2$ in a given event and include the event for the further analysis when P is less than a specified value, which is gradually decreased. With our statistics we are able to reduce the limit for P down to 15 GeV (there are a few hundred of particles in the event), which leaves about 5% from all (unconstrained) events for the most central case. No noticeable effect is detected, therefore the considered correlation measure is not sensitive to the global transverse-momentum conservation.

VI. CONCLUSIONS

The initial shape and the volume of the fireball fluctuate due to the random nature of the Glauber approach. As is well known, the subsequent hydrodynamic evolution carries over the asymmetry of the shape of the fireball into anisotropies of the particle spectra. A similar mechanism, analyzed in detail in this work, transmits the event-by-event fluctuations of the transverse size of the fireball into the fluctuations of the average transverse momentum in each event, as identified in [1]. Here are the main findings of our analysis:

1. The state-of-the-art event-by-event viscous $(3+1)$-D hydrodynamic calculations with fluctuating initial conditions confirm that fluctuations of the mean transverse momentum in each event are generated from the fluctuations of the initial geometry.

2. The amount of scaled transverse momentum fluctuations is determined by the scaled fluctuations of the transverse size of the fireball. We observe an anticorrelation of the initial size of the fireball and of the transverse momentum generated in an event. The expansion of a source of larger extent yields smaller p_T then in the case of a squeezed source, and vice versa.

3. Hydrodynamic expansion is applied to an ensemble of events, corresponding to centralities $0-70\%$ in Au-Au collisions at $\sqrt{s_{NN}} = 200$ GeV. We find a similar magnitude and centrality dependence of the scaled momentum fluctuations $\langle \Delta p_{Ti} \Delta p_{Tj} \rangle / \langle \langle p_T \rangle \rangle$ as in the STAR [32] and PHENIX experiments [29].

4. The dependence of the results on the upper cut-off for the transverse momentum of the particles agrees nicely with the data from the PHENIX Collaboration [29].

5. However, the initial density from the mixed model (wounded nucleons with an admixture of binary collisions), tuned to reproduce the particle multiplicities, yields a visible overprediction of the observed value of $\langle \Delta p_{Ti} \Delta p_{Tj} \rangle / \langle \langle p_T \rangle \rangle$ in the whole centrality range. For most central events the overprediction is at the level of 50%, while it gets relatively closer to the data with increased centrality.

6. Hydrodynamic expansion yields a stronger transverse push and, simultaneously, stronger p_T-fluctuations when the shear viscosity is increased, the freeze-out temperature is lowered, or if the bulk viscosity is lowered. However, the scaled fluctuation measure $\langle \Delta p_{Ti} \Delta p_{Tj} \rangle / \langle \langle p_T \rangle \rangle$ shows very little changes with these modifications of the physical parameters.

7. Predictions of our approach remain essentially unchanged when the core-corona mechanism of particle emission is incorporated. Other effects, such as the transverse-momentum conservation or the finite detector acceptance do not affect the results, either.

The above points indicate that the identified "geometric" mechanism of generating the transverse-momentum fluctuations from the initial Glauber-like model is, on the one hand, very important, easily reproducing the size of the effect and catching the basic features of the data, on the other hand, it is somewhat too strong. That hints on an improvement of the popular Glauber approach of the initial phase. We recall that the calculations using the averaged initial conditions [1] show that the fluctuations of the initial size are reduced if the density in the fireball is determined with the wounded nucleons only, i.e., without the admixture of binary collisions. At the same time, however, the model with the wounded nucleons only fails to generate the proper multiplicity dependence on centrality, thus is less realistic. Moreover, hydrodynamic fluctuations in the evolution could add another source of $\langle p_T \rangle$ fluctuations [103, 104]. Thus, it remains a challenge to understand in detail the earliest phase of the collision and reproduce in a *uniform* way the rich collection of the one-body and the correlation data, including also the harmonic flow.

ACKNOWLEDGMENTS

Supported by Polish Ministry of Science and Higher Education, grant N N202 263438, and National Science Centre, grant DEC-2011/01/D/ST2/00772. Part of the numerical calculations were made on the Cracow Cloud One cluster.

[1] W. Broniowski, M. Chojnacki, and L. Obara, Phys. Rev. **C80**, 051902 (2009)
[2] W. Broniowski, M. Rybczyński, and P. Bożek, Comput. Phys. Commun. **180**, 69 (2009)
[3] P. Bożek, Phys. Rev. **C85**, 034901 (2012)
[4] P. Bożek, Phys. Rev. **C85**, 014911 (2012)
[5] A. Kisiel, T. Tałuć, W. Broniowski, and W. Florkowski, Comput. Phys. Commun. **174**, 669 (2006)
[6] M. Chojnacki, A. Kisiel, W. Florkowski, and W. Broniowski, Comput.Phys.Commun. **183**, 746 (2012)
[7] M. Gaździcki and S. Mrówczyński, Z. Phys. **C54**, 127 (1992)
[8] L. Stodolsky, Phys. Rev. Lett. **75**, 1044 (1995)
[9] E. V. Shuryak, Phys. Lett. **B423**, 9 (1998)
[10] S. Mrówczyński, Phys. Lett. **B430**, 9 (1998)

[11] F. Liu, A. Tai, M. Gazdzicki, and R. Stock, Eur.Phys.J. **C8**, 649 (1999)
[12] S. A. Voloshin, V. Koch, and H. G. Ritter, Phys. Rev. **C60**, 024901 (1999)
[13] G. Baym and H. Heiselberg, Phys. Lett. **B469**, 7 (1999)
[14] S. A. Voloshin (STAR), AIP Conf. Proc. **610**, 591 (2001)
[15] R. Korus, S. Mrówczyński, M. Rybczyński, and Z. Włodarczyk, Phys. Rev. **C64**, 054908 (2001)
[16] S. Gavin, Phys. Rev. Lett. **92**, 162301 (2004)
[17] J. Dias de Deus, E. Ferreiro, C. Pajares, and R. Ugoccioni, Eur.Phys.J. **C40**, 229 (2005)
[18] S. A. Voloshin, Nucl.Phys. **A749**, 287 (2005)
[19] S. Mrówczyński, M. Rybczyński, and Z. Włodarczyk, Phys.Rev. **C70**, 054906 (2004)
[20] M. Abdel-Aziz and S. Gavin, Nucl.Phys. **A774**, 623 (2006)
[21] W. Broniowski, B. Hiller, W. Florkowski, and P. Bożek, Phys.Lett. **B635**, 290 (2006)
[22] D. J. Prindle and T. A. Trainor (STAR Collaboration), PoS **CFRNC2006**, 007 (2006)
[23] S. Gavin and M. Abdel-Aziz, Phys.Rev.Lett. **97**, 162302 (2006)
[24] M. Sharma and C. A. Pruneau, Phys.Rev. **C79**, 024905 (2009)
[25] S. Mrówczyński, Acta Phys.Polon. **B40**, 1053 (2009)
[26] Y. Hama, R. P. G. Andrade, F. Grassi, W. L. Qian, and T. Kodama, Acta Phys. Polon. **B40**, 931 (2009)
[27] J. Adams *et al.* (STAR Collaboration), Phys.Rev. **C71**, 064906 (2005)
[28] D. Adamova *et al.* (CERES Collaboration), Nucl.Phys. **A727**, 97 (2003)
[29] S. Adler *et al.* (PHENIX Collaboration), Phys.Rev.Lett. **93**, 092301 (2004)
[30] T. Anticic *et al.* (NA49 Collaboration), Phys.Rev. **C70**, 034902 (2004)
[31] J. Adams *et al.* (STAR Collaboration), J.Phys.G **G34**, 799 (2007)
[32] J. Adams *et al.* (STAR Collaboration), Phys.Rev. **C72**, 044902 (2005)
[33] J. Adams *et al.* (STAR Collaboration), J.Phys.G **G32**, L37 (2006)
[34] J. Adams *et al.* (STAR Collaboration), J.Phys.G **G34**, 451 (2007)
[35] K. Grebieszkow, C. Alt, T. Anticic, B. Baatar, D. Barna, *et al.*, PoS **CPOD07**, 022 (2007)
[36] T. Anticic *et al.* (NA49), Phys. Rev. **C79**, 044904 (2009)
[37] D. Adamova *et al.* (CERES Collaboration), Nucl.Phys. **A811**, 179 (2008)
[38] H. Agakishiev *et al.* (STAR Collaboration), Phys.Lett. **B704**, 467 (2011)
[39] A. Białas, M. Bleszyński, and W. Czyż, Nucl. Phys. **B111**, 461 (1976)
[40] A. Bialas, J. Phys. **G35**, 044053 (2008)
[41] D. Kharzeev and M. Nardi, Phys. Lett. **B507**, 121 (2001)
[42] C. E. Aguiar, T. Kodama, T. Osada, and Y. Hama, J. Phys. **G27**, 75 (2001)
[43] M. Miller and R. Snellings(2003), nucl-ex/0312008
[44] R. S. Bhalerao, J.-P. Blaizot, N. Borghini, and J.-Y. Ollitrault, Phys. Lett. **B627**, 49 (2005)
[45] S. Manly *et al.* (PHOBOS), Nucl. Phys. **A774**, 523 (2006)
[46] B. Alver *et al.* (PHOBOS), Phys. Rev. Lett. **98**, 242302 (2007)
[47] R. Andrade, F. Grassi, Y. Hama, T. Kodama, and J. Socolowski, O., Phys. Rev. Lett. **97**, 202302 (2006)
[48] S. A. Voloshin(2006), arXiv:nucl-th/0606022
[49] H. J. Drescher and Y. Nara, Phys. Rev. **C75**, 034905 (2007)
[50] W. Broniowski, P. Bożek, and M. Rybczyński, Phys. Rev. **C76**, 054905 (2007)
[51] Y. Hama, R. Peterson G.Andrade, F. Grassi, W.-L. Qian, T. Osada, *et al.*, Phys.Atom.Nucl. **71**, 1558 (2008)
[52] S. A. Voloshin, A. M. Poskanzer, A. Tang, and G. Wang, Phys. Lett. **B659**, 537 (2008)
[53] R. P. G. Andrade *et al.*, Acta Phys. Polon. **B40**, 993 (2009)
[54] B. Alver and G. Roland, Phys. Rev. **C81**, 054905 (2010)
[55] B. H. Alver, C. Gombeaud, M. Luzum, and J.-Y. Ollitrault, Phys. Rev. **C82**, 034913 (2010)
[56] H. Petersen, G.-Y. Qin, S. A. Bass, and B. Muller, Phys.Rev. **C82**, 041901 (2010)
[57] P. Bożek, W. Broniowski, and J. Moreira, Phys.Rev. **C83**, 034911 (2011)
[58] D. Teaney and L. Yan, Phys. Rev. **C83**, 064904 (2011)
[59] F. G. Gardim, F. Grassi, Y. Hama, M. Luzum, and J.-Y. Ollitrault, Phys. Rev. **C83**, 064901 (2011)
[60] B. B. Back *et al.* (PHOBOS), Phys. Rev. **C65**, 031901 (2002)
[61] B. B. Back *et al.* (PHOBOS), Phys. Rev. **C70**, 021902 (2004)
[62] M. Rybczynski and W. Broniowski, Phys.Rev. **C84**, 064913 (2011), 8 pages, 7 figures
[63] A. Białas and W. Czyż, Acta Phys. Polon. **B36**, 905 (2005)
[64] P. Bożek and I. Wyskiel, Phys. Rev. **C81**, 054902 (2010)
[65] P. Bożek, Phys. Rev. **C83**, 044910 (2011)
[66] P. Bożek, Phys. Lett. **B699**, 283 (2011)
[67] A. Białas and A. Bzdak, Phys. Lett. **B649**, 263 (2007)
[68] M. Alvioli, H.-J. Drescher, and M. Strikman, Phys.Lett. **B680**, 225 (2009)
[69] W. Broniowski and M. Rybczynski, Phys.Rev. **C81**, 064909 (2010)
[70] M. Alvioli and M. Strikman, Phys.Rev. **C83**, 044905 (2011)
[71] P. F. Kolb and U. W. Heinz, in *Quark Gluon Plasma 3*, edited by R. Hwa and X. N. Wang (World Scientific, Singapore, 2004) p. 634, arXiv:nucl-th/0305084
[72] P. Huovinen and P. V. Ruuskanen, Ann. Rev. Nucl. Part. Sci. **56**, 163 (2006)
[73] W. Florkowski, *Phenomenology of Ultra-Relativistic Heavy-Ion Collisions* (World Scientific Publishing Company, Singapore, 2010)
[74] K. Werner *et al.*, J. Phys. **G36**, 064030 (2009)
[75] H. Holopainen, H. Niemi, and K. J. Eskola, Phys.Rev. **C83**, 034901 (2011)
[76] F. G. Gardim, F. Grassi, M. Luzum, and J.-Y. Ollitrault, Phys. Rev. **C85**, 024908 (2012)
[77] B. Schenke, S. Jeon, and C. Gale, Phys. Rev. Lett. **106**, 042301 (2011)
[78] Z. Qiu and U. W. Heinz(2011), arXiv:1108.1714 [nucl-th]
[79] A. Chaudhuri(2011), arXiv:1112.1166 [nucl-th]
[80] W. Israel and J. Stewart, Annals Phys. **118**, 341 (1979)
[81] P. Romatschke, Int. J. Mod. Phys. **E19**, 1 (2010)
[82] D. A. Teaney(2009), arXiv:0905.2433 [nucl-th]

[83] S. Borsanyi *et al.*, JHEP **11**, 077 (2010)
[84] M. Chojnacki and W. Florkowski, Acta Phys. Polon. **B38**, 3249 (2007)
[85] W. Broniowski and W. Florkowski, Phys.Rev. **C65**, 024905 (2002)
[86] W. Broniowski, A. Baran, and W. Florkowski, Acta Phys. Polon. **B33**, 4235 (2002)
[87] G. Torrieri *et al.*, Comput. Phys. Commun. **167**, 229 (2005)
[88] D. Teaney, Phys. Rev. **C68**, 034913 (2003)
[89] S. Gavin, Nucl. Phys. **A435**, 826 (1985)A. Hosoya and K. Kajantie, *ibid.* **B250**, 666 (1985)C. Sasaki and K. Redlich, Phys. Rev. **C79**, 055207 (2009)
[90] P. Bożek, Phys. Rev. **C81**, 034909 (2010)
[91] A. Andronic, P. Braun-Munzinger, and J. Stachel, Nucl. Phys. **A772**, 167 (2006)
[92] S. S. Adler *et al.* (PHENIX), Phys. Rev. **C69**, 034909 (2004)
[93] R. Andrade, F. Grassi, Y. Hama, T. Kodama, and W. Qian, Phys.Rev.Lett. **101**, 112301 (2008)
[94] J.-Y. Ollitrault, Phys.Lett. **B273**, 32 (1991)
[95] W. Broniowski, M. Rybczynski, L. Obara, and M. Chojnacki, Acta Phys.Polon.Supp. **3**, 513 (2010)
[96] W. Broniowski, P. Bożek, W. Florkowski, and B. Hiller, PoS **CFRNC2006**, 020 (2006)
[97] E. Retinskaya, M. Luzum, and J.-Y. Ollitrault(2012), arXiv:1203.0931 [nucl-th]
[98] C. Hohne, F. Puhlhofer, and R. Stock, Phys. Lett. **B640**, 96 (2006)
[99] F. Becattini and J. Manninen, Phys. Lett. **B673**, 19 (2009)
[100] P. Bożek, Acta Phys. Polon. **B36**, 3071 (2005)
[101] K. Werner, Phys. Rev. Lett. **98**, 152301 (2007)
[102] P. Bożek, Phys. Rev. **C79**, 054901 (2009)
[103] S. Florchinger and U. A. Wiedemann, JHEP **11**, 100 (2011)
[104] J. Kapusta, B. Mueller, and M. Stephanov(2012), arXiv:1201.3405 [nucl-th]